Supplementary information

Cancer-associated mutations of histones H2B, H3.1, and H2A.Z.1 affect the structure and stability of the nucleosome

Yasuhiro Arimura[1,2], Masae Ikura[3], Risa Fujita[1,2], Mamiko Noda[2], Wataru Kobayashi1[1,2], Naoki Horikoshi[2], Jiying Sun[4], Lin Shi[4], Masayuki Kusakabe[5], Masahiko Harata[5], Yasuyuki Ohkawa[6], Satoshi Tashiro[4], Hiroshi Kimura[7], Tsuyoshi Ikura[3], and Hitoshi Kurumizaka[1,2]*

[1] Laboratory of Chromatin Structure and Function, Institute for Quantitative Biosciences, The University of Tokyo, 1-1-1 Yayoi, Bunkyo-ku, Tokyo 113-0032, Japan.
[2] Laboratory of Structural Biology, Graduate School of Advanced Science and Engineering, Waseda University, 2-2 Wakamatsu-cho, Shinjuku-ku, Tokyo 162-8480, Japan.
[3] Laboratory of Chromatin Regulatory Network, Department of Genome Biology,Radiation Biology Center, Graduate School of Biostudies, Kyoto University, Yoshidakonoe, Sakyo-ku, Kyoto 606-8501, Japan.
[4] Department of Cellular Biology, Research Institute for Radiation Biology and Medicine, Hiroshima University, 1-2-3 Kasumi, Minami-ku, Hiroshima 734-8553, Japan.
[5] Laboratory of Molecular Biology, Graduate School of Agricultural Science, Tohoku University, Aoba-ku, 468-1 Aoba, Aramaki, Aoba-ku, Sendai 980-0845, Japan.
[6] Division of Transcriptomics, Medical Institute of Bioregulation, Kyushu University, 3-1-1 Maidashi, Higashi-ku, Fukuoka 812-8582, Japan.
[7] Cell Biology Center, Institute of Innovative Research, Tokyo Institute of Technology, 4259 Nagatsuta-cho, Midori-ku, Yokohama 226-8503, Japan.

* To whom correspondence should be addressed. Tel: 03-5841-7826; Fax: 03-5841-1468; Email: kurumizaka@iam.u-tokyo.ac.jp

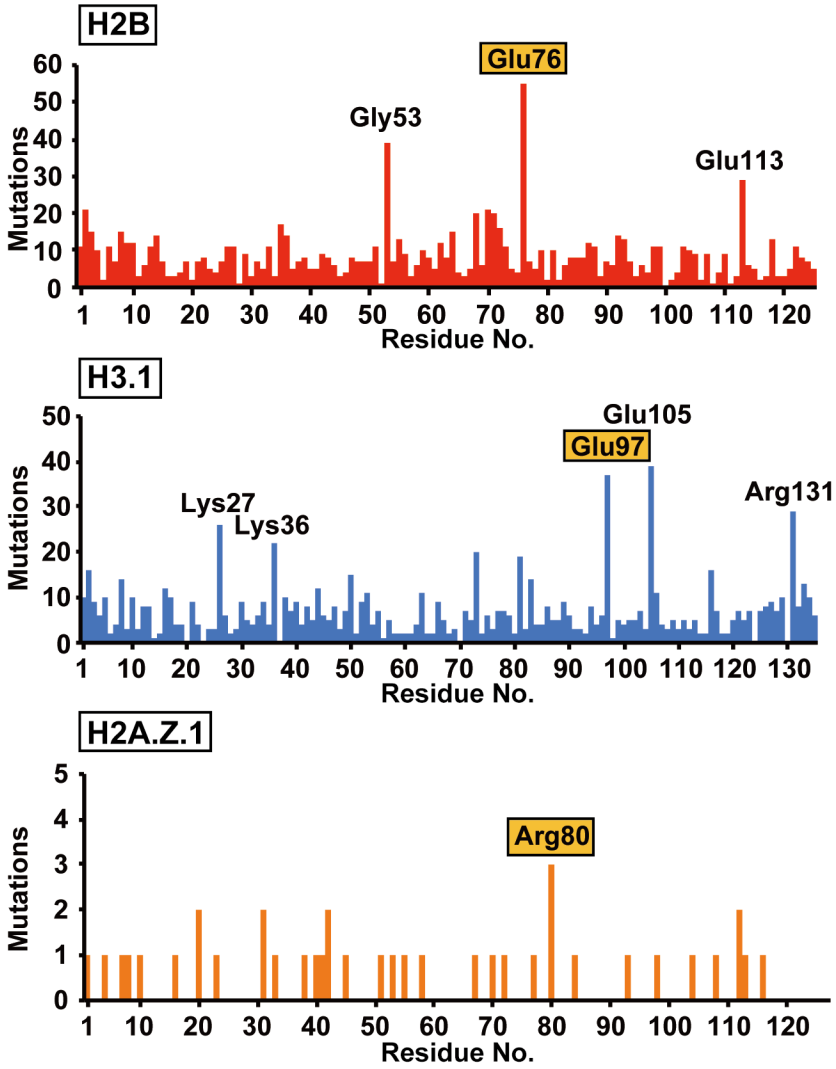

Figure S1. Missense mutations in *H2B*, *H3.1*, and *H2A.Z.1* genes in human cancer cells. The numbers of patients carrying a missense mutation in a gene encoding H2B, H3.1, or H2A.Z.1 are plotted against the amino acid residues. Mutation data were collected from the cBioPortal (34, 35) on July 4th, 2018. The yellow boxes show the mutations analyzed in the present study.

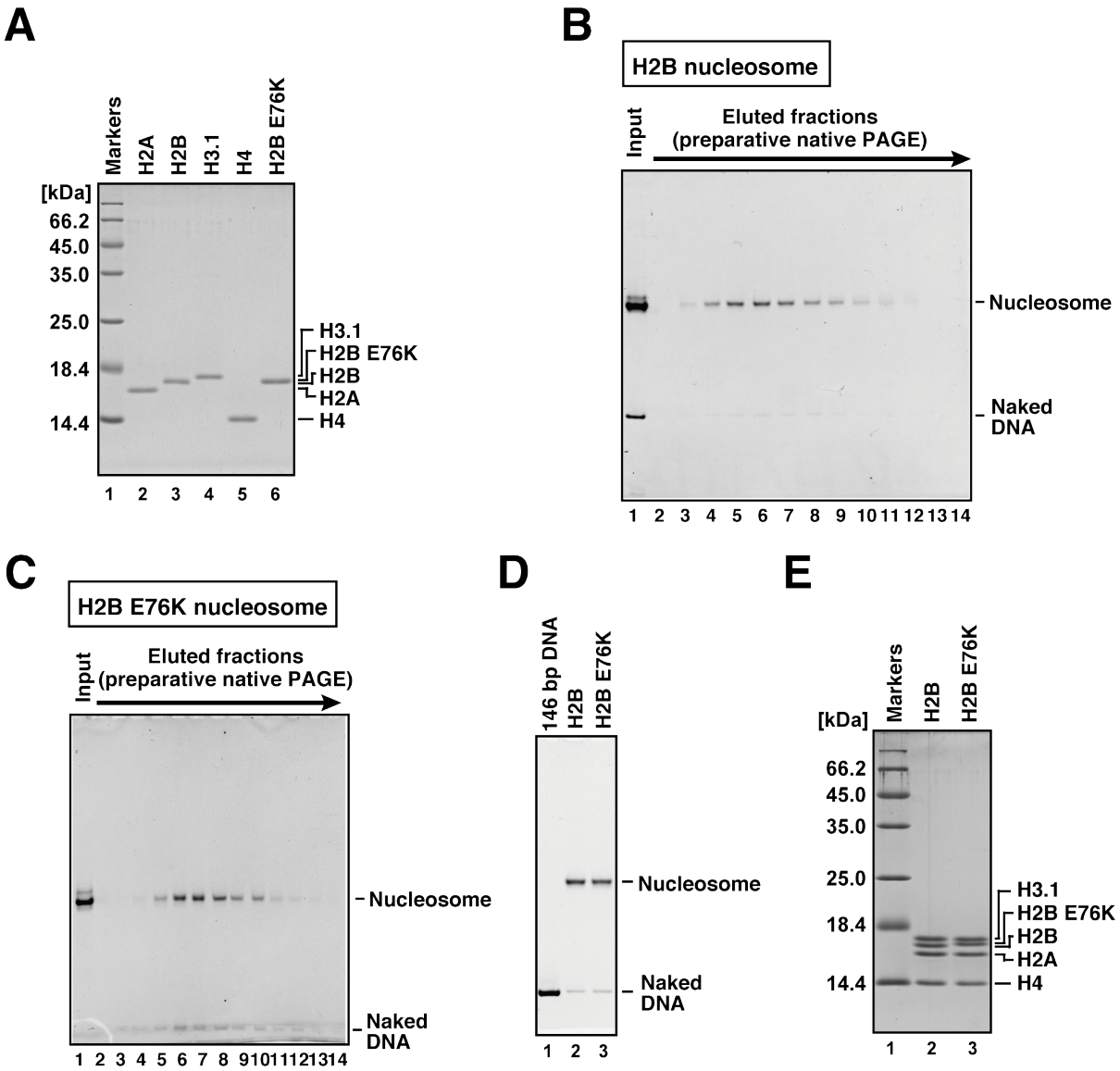

Figure S2. Preparation of the H2B and H2B E76K nucleosomes. (A) H2A, H2B, H3.1, H4, and H2B E76K (lanes 2, 3, 4, 5, and 6, respectively) were analyzed by 18% SDS-PAGE with CBB staining. (B, C) The reconstituted H2B nucleosome and H2B E76K nucleosome (lane 1) were purified by native polyacrylamide gel electrophoresis, using a Prep Cell apparatus. The purified nucleosome fractions (lanes 2-14) were analyzed by 6% native PAGE with ethidium bromide staining. The fractions containing the H2B nucleosome (B, lanes 5-10) and the H2B E76K nucleosome (C, lanes 6-10) were collected. (D) The purified H2B wild-type (lane 2), and H2B E76K (lane 3) nucleosomes were analyzed by 6% native PAGE with ethidium bromide staining. (E) The histone compositions of the H2B wild-type (lane 2) and H2B E76K (lane 3) nucleosomes were analyzed by 18% SDS-PAGE with CBB staining.

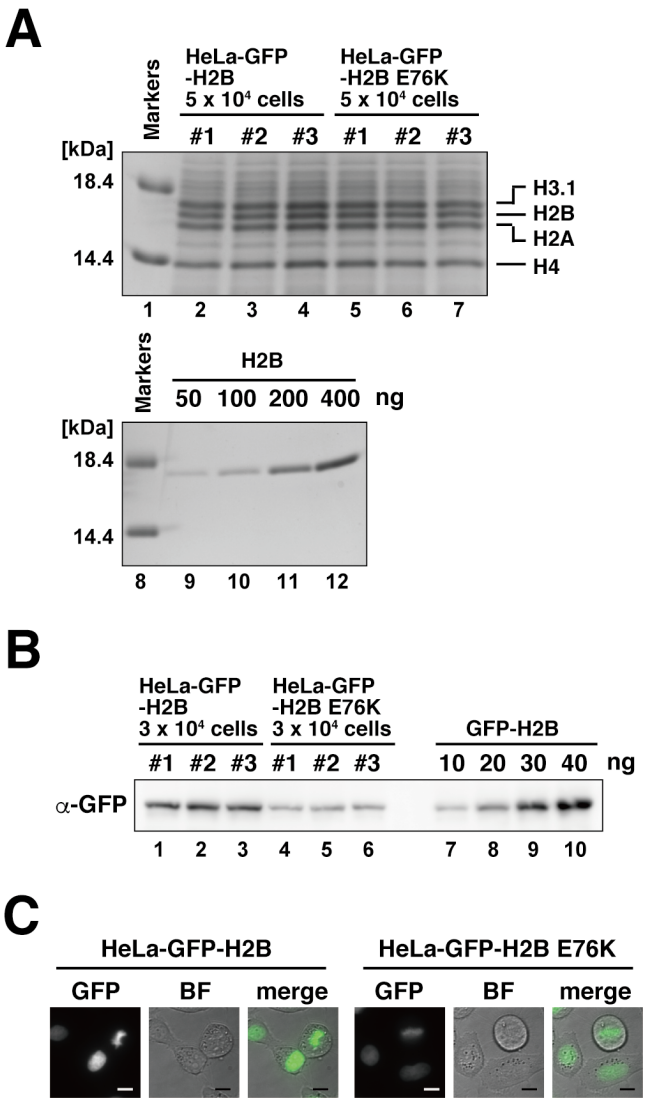

Figure S3. GFP-H2B and GFP-H2B E76K production in HeLa cells. (A) Levels of histones in HeLa cells expressing GFP-H2B and GFP-H2B E76K. Three independent whole cell lysates (#1-#3) were prepared from HeLa cells producing GFP-H2B (lanes 2-4) and GFP-H2B E76K (lanes 5-7), and were analyzed by SDS-PAGE and CBB staining. The amounts of H2B in 5 × 10^4 cells were estimated to be 307 and 260 ng for cells producing GFP-H2B and GFP-H2B E76K, respectively, by using the calibration curve obtained from known amounts (50, 100, 200, and 400 ng) of recombinant H2B (lanes 9-12). The full gel image is shown in Fig. S13G. (B) Levels of GFP-H2B and GFP-H2B E76K. The same lysates used in A (3.0 × 10^4 equivalent) were separated by SDS-PAGE and analyzed by western blotting. The GFP-H2B (lanes 1-3) and GFP-H2B E76K (lanes 4-6) levels in HeLa cells were estimated to be 25 and 14 ng, respectively, by using the calibration curve from the known amounts (10, 20, 30, and 40 ng) of recombinant GFP-H2B (lanes 7-10). From these data, the amounts of GFP-H2B and GFP-H2B E76K in stably expressing cells were calculated to be 14% and 9% of the endogenous H2B, respectively. The full image of the western blot is shown in Fig. S13H. (C) Localization of GFP-H2B and GFP-H2B E76K in interphase and mitotic HeLa cells. Fluorescent (GFP) and bright-field (BF) images are shown with the merged images (merge). Both GFP-H2B and GFP-H2B E76K are localized to the nucleus and chromosomes in interphase and mitotic cells, respectively. Bars, 10 μm.

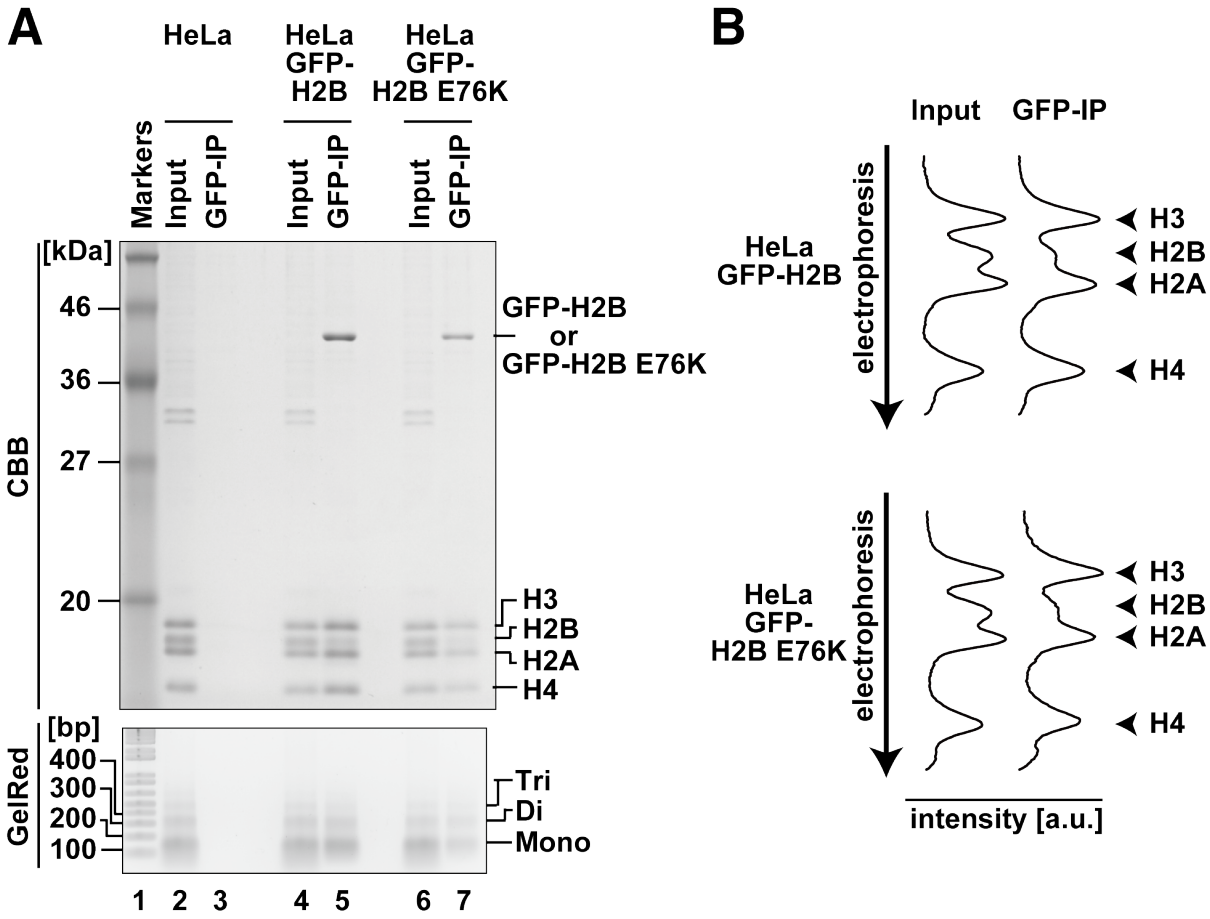

Figure S4. GFP-H2B and GFP-H2B E76K are incorporated into nucleosomes in HeLa cells. (A) Pull-down analyses of GFP-tagged histones, prepared from the micrococcal nuclease digested HeLa cell chromatin containing GFP-H2B or GFP-H2B E76K. Upper panel: SDS-PAGE analysis with CBB staining. Lower panel: agarose gel electrophoresis with GelRed staining. Lanes 2, 4, and 6 indicate the micrococcal nuclease digested chromatin fractions from HeLa cells, HeLa cells producing GFP-H2B, and HeLa cells producing GFP-H2B E76K, respectively. Lanes 3, 5, and 7 indicate the pull-down fractions with GFP-Trap beads, using micrococcal nuclease digested chromatin fractions from HeLa cells, HeLa cells producing GFP-H2B, and HeLa cells producing GFP-H2B E76K, respectively. The full gel image of the agarose gel electrophoresis is shown in Fig. S13I. (B) Densitometric intensity profiles of the SDS-PAGE gel shown Fig. S3A. The micrococcal nuclease digested chromatin fraction (Fig. S4A lanes 4 and 6) and the pulled-down fraction (Fig. S4A lanes 5 and 7) were scanned. HeLa cells producing GFP-H2B (upper panel) and GFP-H2B E76K (lower panel) are presented.

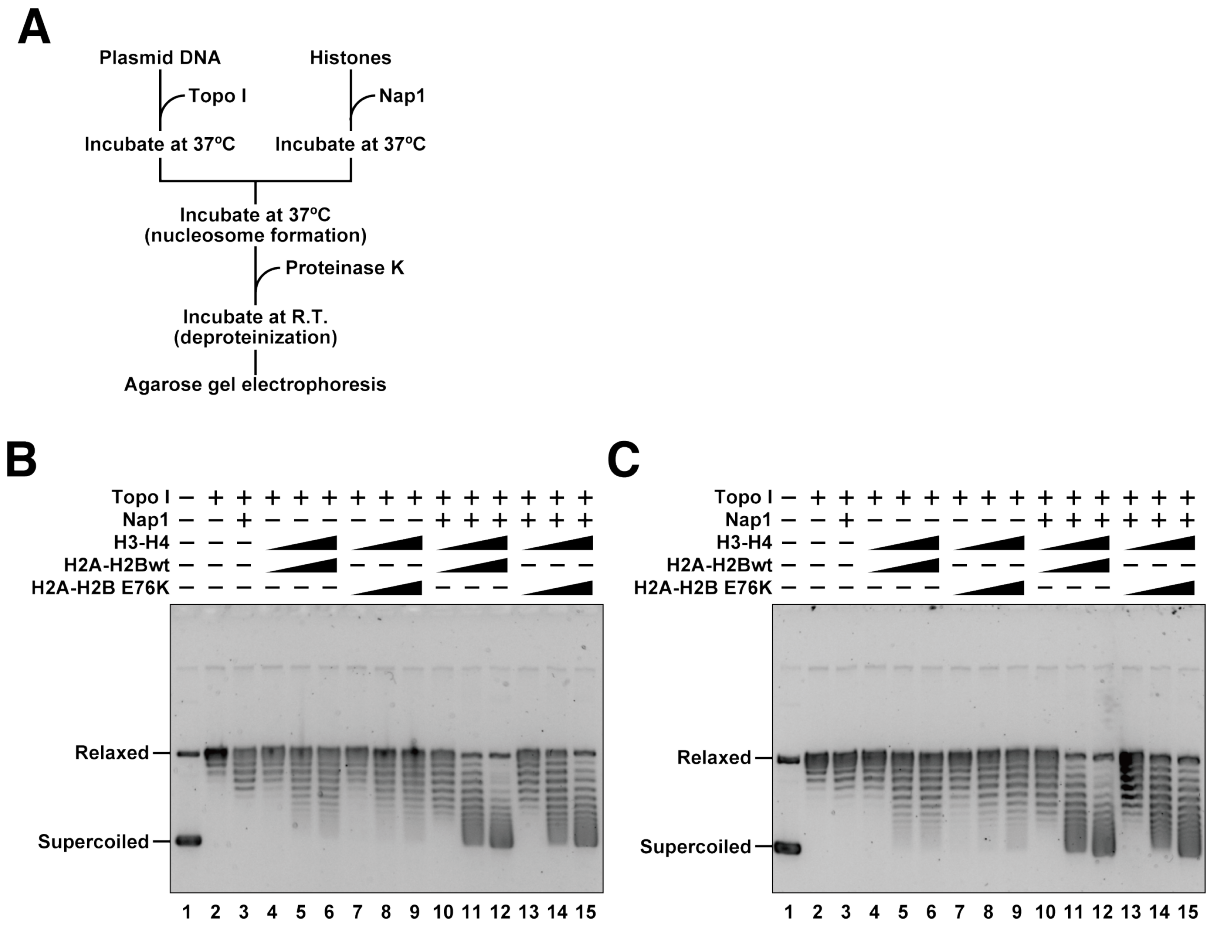

Figure S5. Nucleosome assembly assay with the histone chaperone, Nap1, with wild-type H2B and the H2B E76K mutant. (A) Schematic representation of the nucleosome assembly assay. (B, C) Two independent experiments of the nucleosome assembly assay were performed. The results were reproducible.

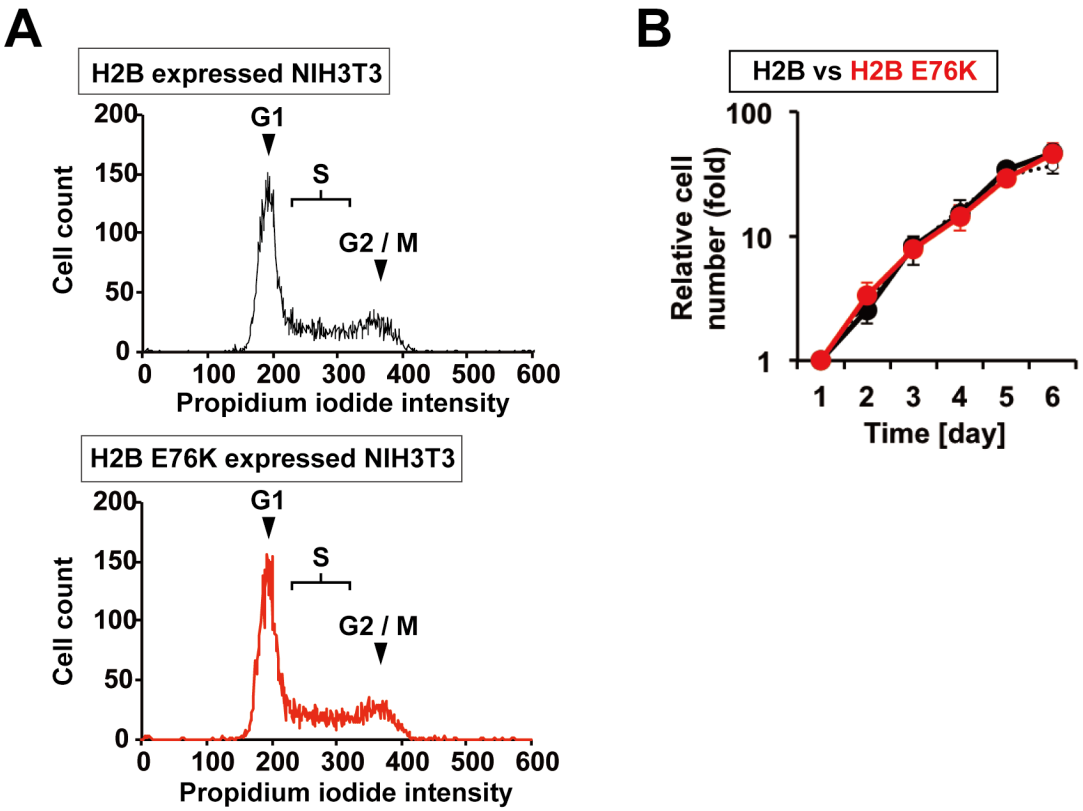

Figure S6. (A) Cell cycle analysis of NIH3T3 cells producing H2B or H2B E76K. Upper and lower panels indicate the histograms of DNA contents in the NIH3T3 cells producing H2B and H2B E76K, respectively. The DNA contents in each cell type were quantified by the propidium iodide staining method. (B) Cell growth rates of NIH3T3 cells producing H2B or H2B E76K. Black and red lines indicate the growth curves of the NIH3T3 cells producing H2B and H2B E76K, respectively. The black dotted line indicates the growth curve of NIH3T3 cells transfected with the empty pCAGGS-IRES-GFP plasmid. Three independent experiments were performed, and the average values are plotted against the days after transfection, as graphs with the standard deviations.

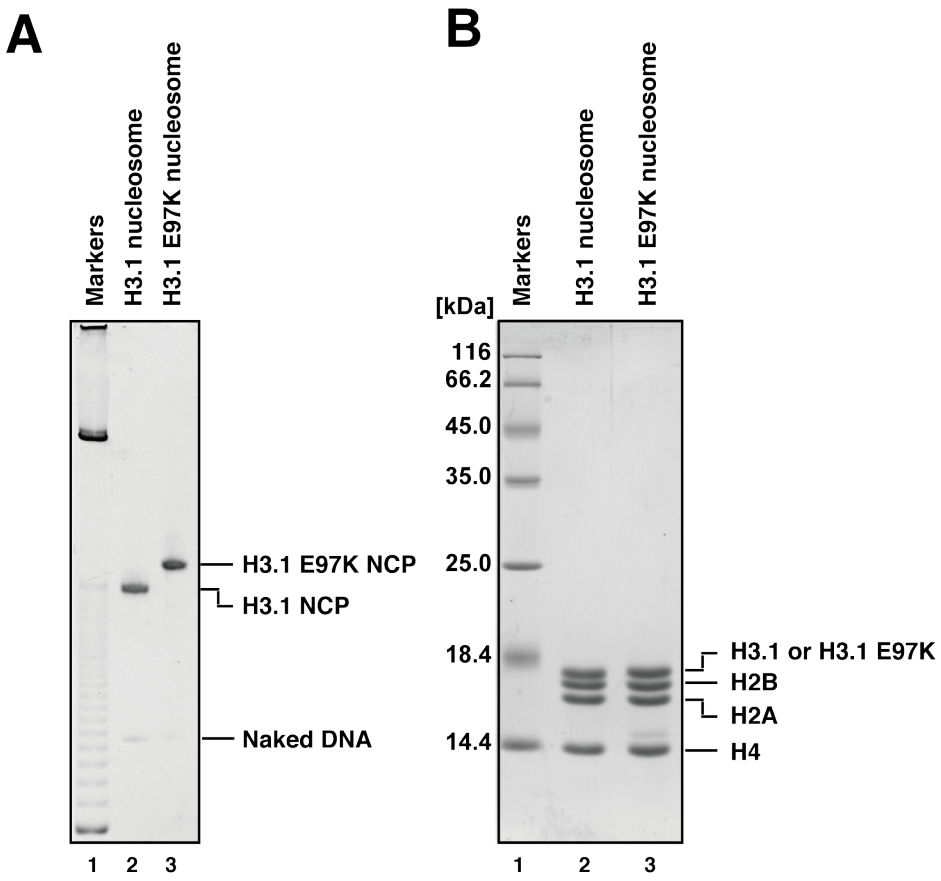

Figure S7. Preparation of the H3.1 E97K nucleosome. (A) The purified H3.1 wild-type (lane 2) and H3.1 E97K (lane 3) nucleosomes were analyzed by 6% native PAGE with ethidium bromide staining. (B) The histone compositions of the H3.1 wild-type (lane 2) and H3.1 E97K (lane 3) nucleosomes were analyzed by 18% SDS-PAGE with CBB staining.

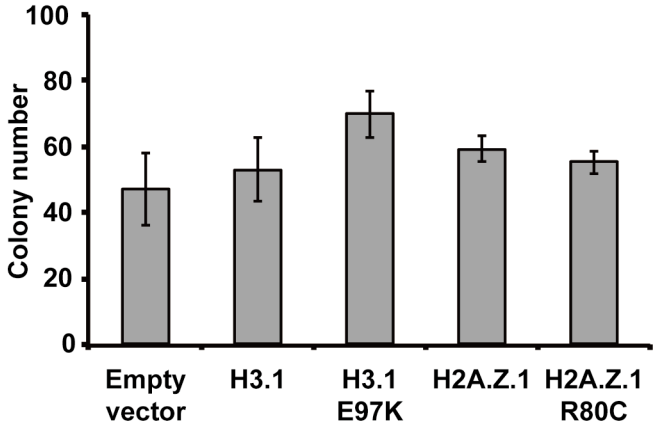

Figure S8. Colony formation assay with NIH3T3 cells expressing H3.1, H3.1 E97K, H2A.Z.1, or H2A.Z.1 R80C. The colony numbers of cells expressing H3.1, H3.1 E97K, H2A.Z.1, or H2A.Z.1 R80C are plotted. Three independent experiments were performed, and the average colony numbers are presented as bar graphs with the standard deviations (*n*=3).

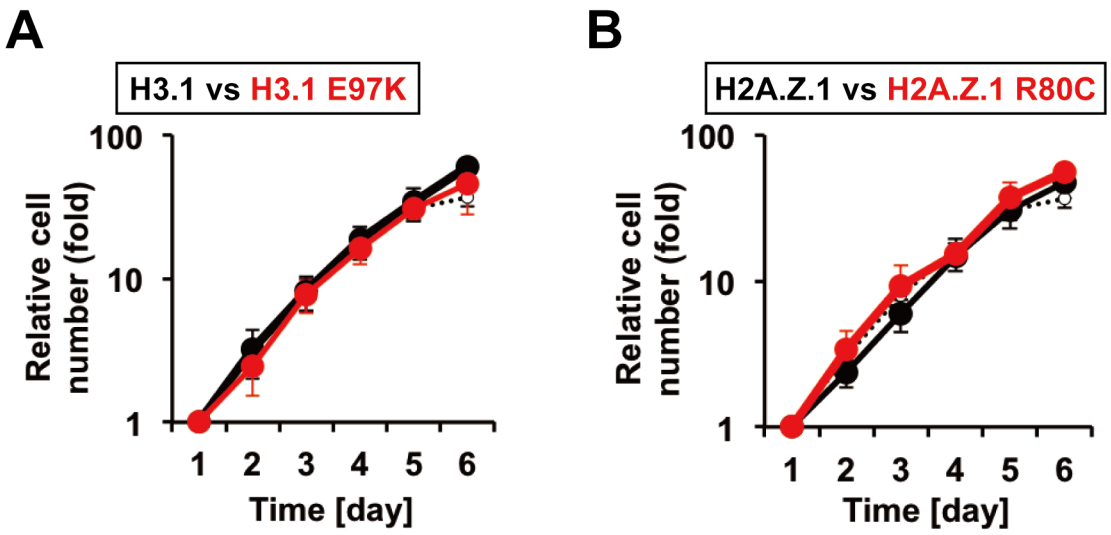

Figure S9. Cell growth rate analyses of NIH3T3 cells producing histone mutants. (A) Black and red lines indicate the growth curves of the NIH3T3 cells producing H3.1 and H3.1 E97K, respectively. (B) Black and red lines indicate the growth curves of the NIH3T3 cells producing H2A.Z.1 and H2A.Z.1 R80C, respectively. Black dotted lines indicate the growth curves of the NIH3T3 cells transfected with the empty pCAGGS-IRES-GFP plasmid. Three independent experiments were performed, and the average values are plotted against the days after transfection, as graphs with the standard deviations.

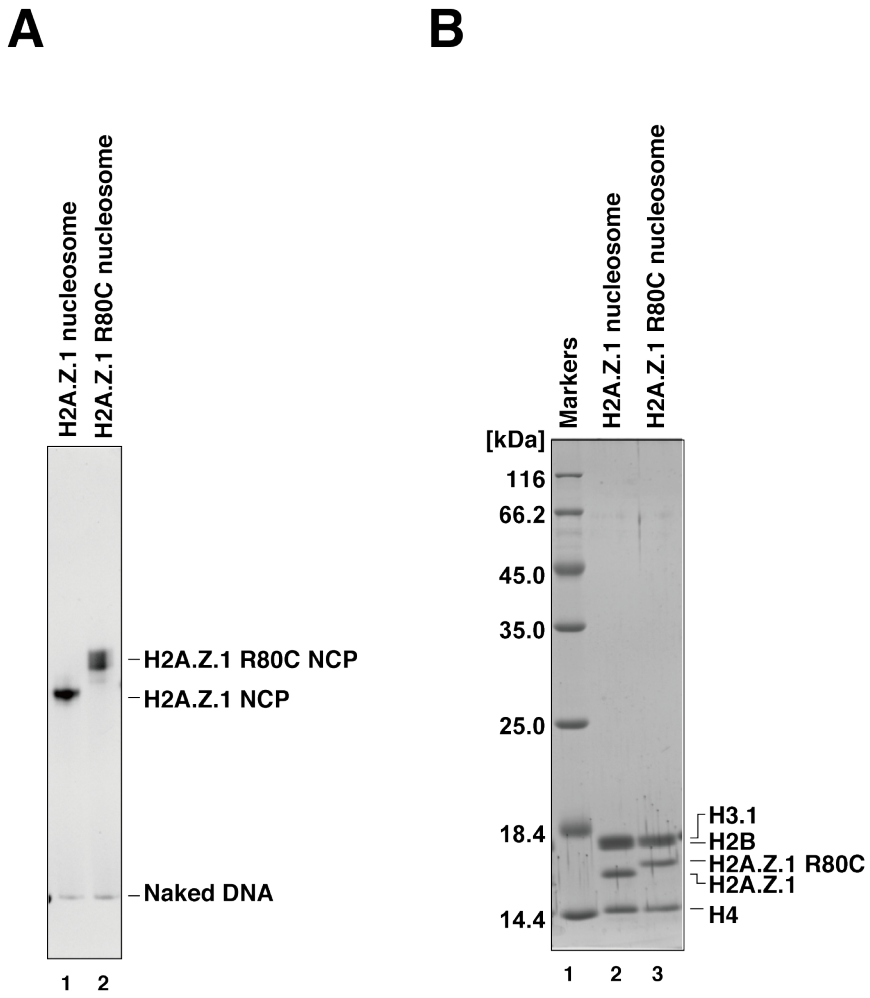

Figure S10. Preparation of the H2A.Z.1 R80C nucleosome. (A) The purified H2A.Z.1 wild-type (lane 1) and H2A.Z.1 R80C (lane 2) nucleosomes were analyzed by 6% native PAGE with ethidium bromide staining. (B) The histone compositions of the H2A.Z.1 wild-type (lane 2) and H2A.Z.1 R80C (lane 3) nucleosomes were analyzed by 18% SDS-PAGE with CBB staining.

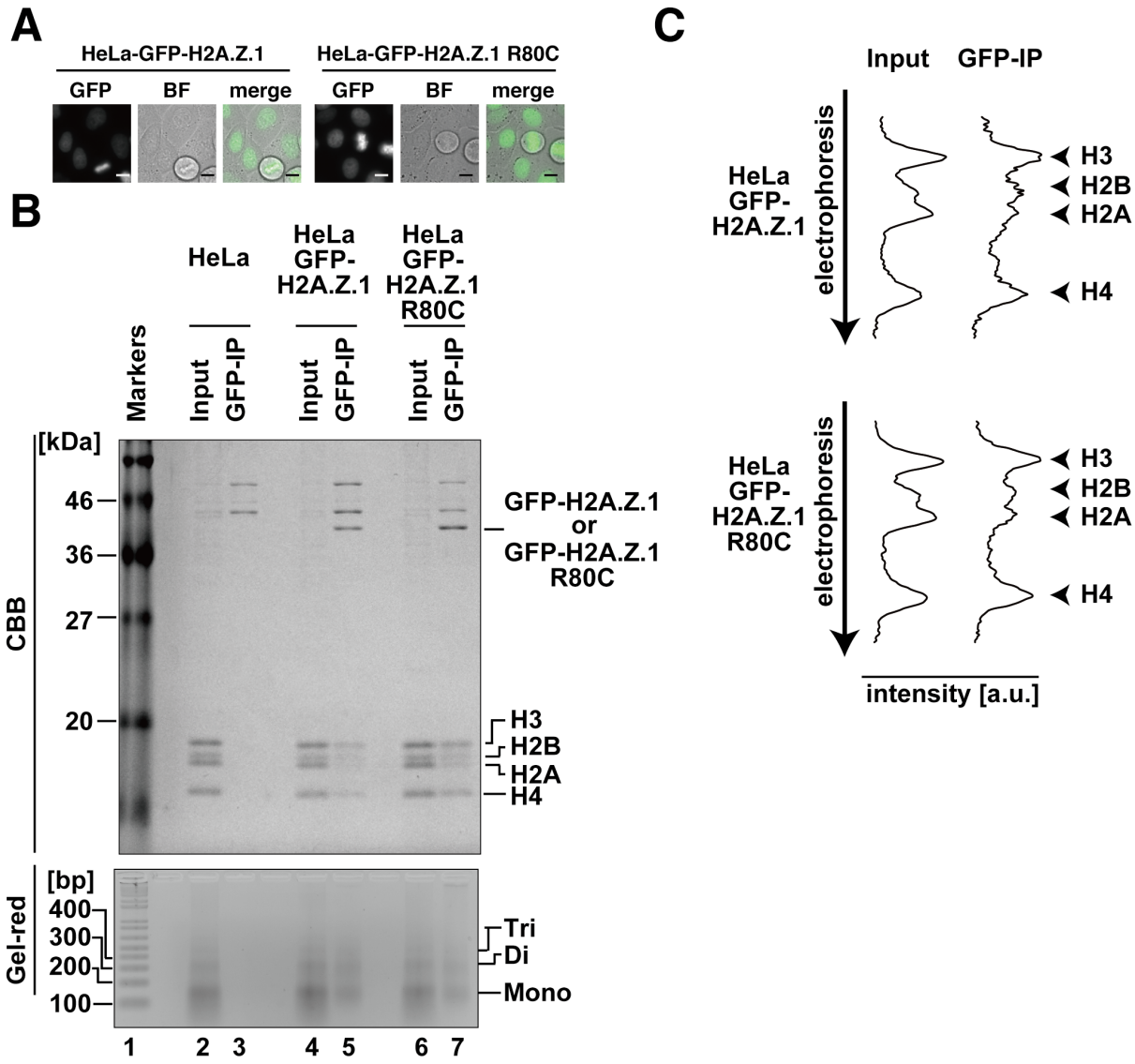

Figure S11. GFP-H2A.Z and GFP-H2A.Z R80C are incorporated into nucleosomes in HeLa cells. (A) Localization of GFP-H2A.Z.1 and GFP-H2A.Z.1 R80C in interphase and mitotic HeLa cells. Fluorescent (GFP) and bright-field (BF) images are shown with the merged images (merge). Both GFP-H2A.Z.1 and GFP-H2A.Z.1 R80C are localized within the nucleus and chromosomes in interphase and mitotic cells, respectively. Bars, 10 µm. (B) Pull-down analyses of GFP-tagged histones, prepared from the micrococcal nuclease digested HeLa cell chromatin containing GFP-H2A.Z.1 or GFP-H2A.Z.1 R80C. Upper panel: SDS-PAGE analysis with CBB staining. Lower panel: agarose gel electrophoresis with GelRed staining. Lanes 2, 4, and 6 indicate the micrococcal nuclease digested chromatin fractions from HeLa cells, HeLa cells producing GFP-H2A.Z.1, and HeLa cells producing GFP-H2A.Z.1 R80C, respectively. Lanes 3, 5, and 7 indicate the pull-down fractions with GFP-Trap beads, using micrococcal nuclease digested chromatin fractions from HeLa cells, HeLa cells producing GFP-H2A.Z.1, and HeLa cells producing GFP-H2A.Z.1 R80C, respectively. The full images of the SDS-PAGE and the agarose gel electrophoresis gels are shown in Fig. S13J and S13K, respectively. (C) Densitometric intensity profiles of the SDS-PAGE gel shown Fig. S11B. The micrococcal nuclease digested chromatin fraction (Fig. 11B lanes 4 and 6) and the pulled-down fraction (Fig. S11B lanes 5 and 7) were scanned. HeLa cells producing GFP-H2A.Z.1 (upper panel) and GFP-H2A.Z.1 R80C (lower panel) are presented.

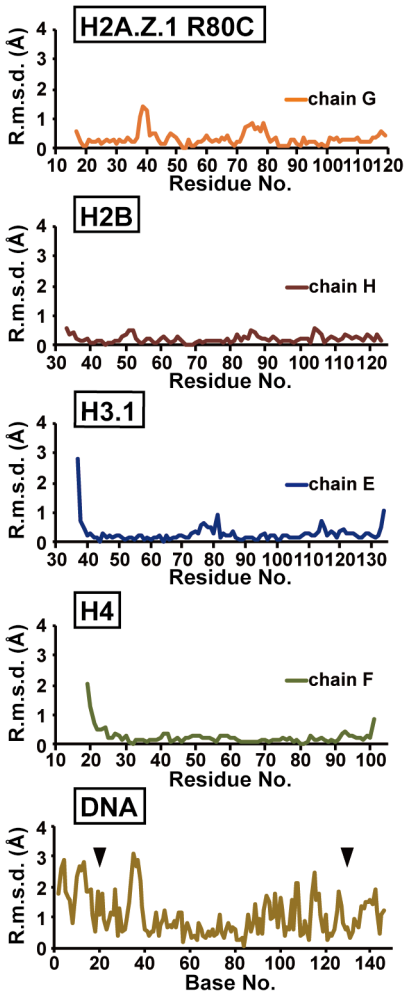

Figure S12. Structural comparison between the H2A.Z.1 R80C nucleosome and the H2A.Z.1 nucleosome (3WA9). The root mean square deviation (r.m.s.d.) values between the corresponding Cα and P atoms of the H2A.Z.1 R80C and wild-type H2A.Z.1 molecules in the nucleosomes are plotted against the amino acid residues and the nucleotides, respectively. In these comparisons, one of the two peptide chains, G, H, E, and F, of the nucleosome with H2A.Z.1 R80C was used. Arrowheads indicate the DNA region contacting the H2A.Z.1 Cys80 residues in the H2A.Z.1 R80C nucleosome.

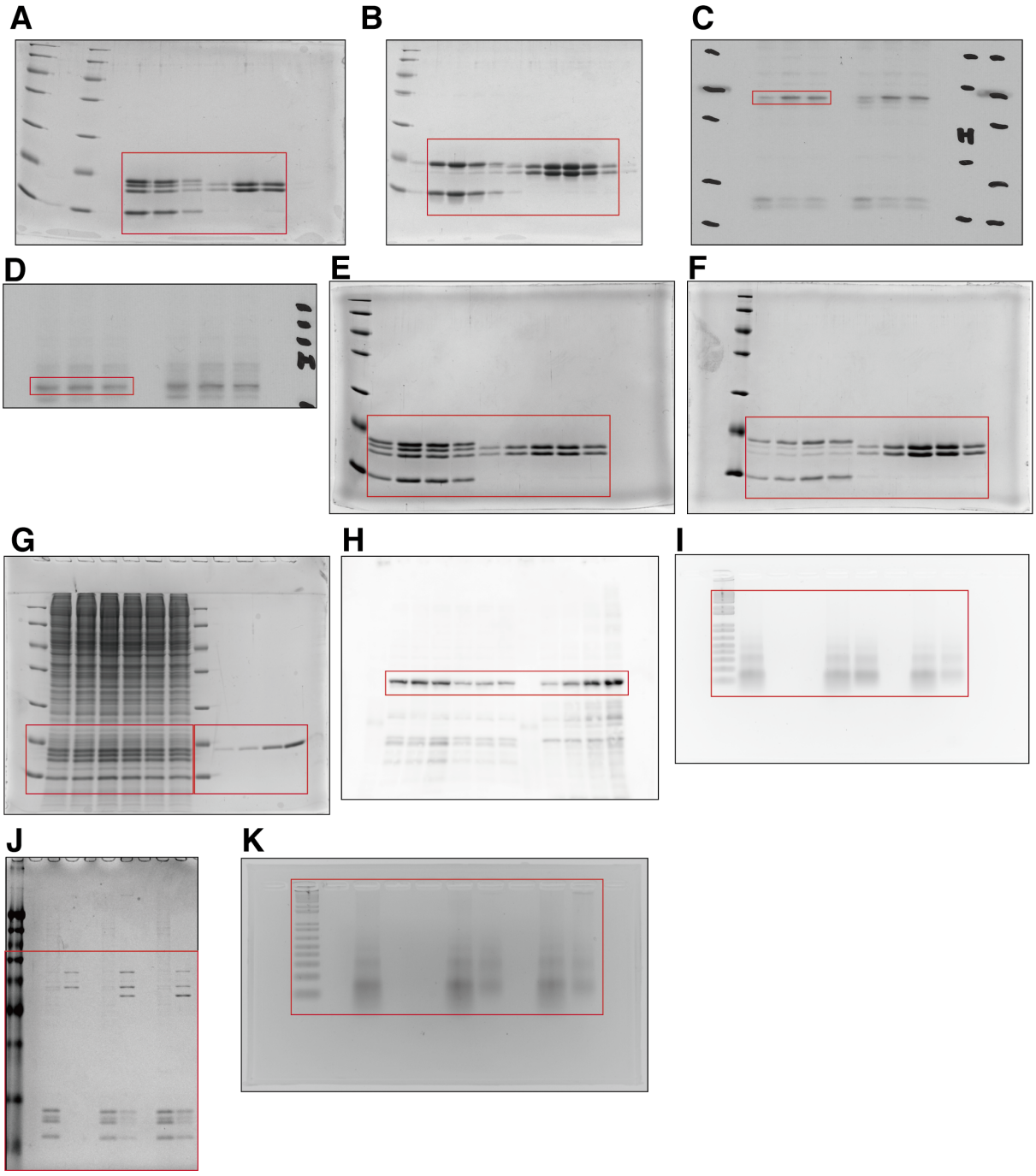

Figure S13. Full images. (A) The full image of Fig. 3B. (B) The full image of Fig. 3C. (C) The full image of Fig. 5C upper panel. (D) The full image of Fig. 5C lower panel. (E) The full image of Fig. 6C. (F) The full image of Fig. 6D. (G) The full image of Fig. S3A. (H) The full image of Fig. S3B. (I) The full image of Fig. S4A lower panel. (J) The full image of Fig. S4A upper panel. (K) The full image of Fig. S11A lower panel. Red rectangles show the areas used in the figures.

Table S1. Data collection and refinement statistics

	H2B E76K nucleosome	H2B wild type nucleosome	H2A.Z.1 R80C nucleosome
Data collection			
Space group	$P2_12_12_1$	$P2_12_12_1$	$P2_12_12_1$
Cell dimensions			
a, *b*, *c* (Å)	98.992 107.316 167.719	98.913, 107.103, 167.003	99.399, 108.332, 170.902
α, β, γ (°)	90.000, 90.000, 90.000	90.000, 90.000, 90.000	90.000, 90.000, 90.000
Resolution (Å)	50.00-1.98 (2.05-1.98)	20.00-2.08 (2.15-2.08)	50.00-2.44 (2.53-2.44)
R_{merge} (%)	7.2 (48.8)	10.0 (48.7)	9.2 (41.5)
I / σI	19.4 (2.5)	17.7 (2.6)	23.3 (2.0)
Completeness (%)	96.9 (91.5)	98.5 (91.2)	97.8 (92.1)
$CC_{1/2}$ in outer shell	0.698	0.685	0.577
Redundancy	7.1 (3.5)	8.7 (5.4)	5.0 (3.0)
Refinement			
Resolution (Å)	49.582 - 1.990	20.000 - 2.087	49.700 - 2.450
No. reflections	118684	103642	66581
R_{work} / R_{free} (%)	21.06 / 25.21	20.19 / 24.92	20.05 / 24.35
No. atoms			
Protein	5980	6001	5952
DNA	5980	5962	5980
ion	14	14	13
Water	509	413	60
B-factors			
Protein	31.9	31.9	49.6
DNA	53.8	50.5	73.8
ion	45.6	43.5	75.0
Water	35.2	33.2	45.1
R.m.s. deviations			
Bond lengths (Å)	0.011	0.006	0.008
Bond angles (°)	1.290	0.882	1.080
Ramachandran plot statistics			
Favored (%)	99.46	98.51	98.78
Allowed (%)	0.54	1.49	1.22
Outliers (%)	0.00	0.00	0.00

*Values in parentheses are for highest-resolution shell.